WIND TUNNEL TESTS TO EVALUATE THE RAIN DROPS DEVIATIONS AROUND DIFFERENT TYPES OF PRECIPITATION GAUGES

Mattia Stagnaro [1,2], Arianna Cauteruccio [1,2], Elia Brambilla [3], Luca G. Lanza [1,2*] & Daniele Rocchi [3]

(1) Department of Civil, Chemical and Environmental Engineering, University of Genova, Genoa, Italy
(2) WMO/CIMO Lead Centre "B. Castelli" on Precipitation Intensity, Italy
(3) Department of Mechanical Engineering, Politecnico di Milano, Milan, Italy

**email: luca.lanza@unige.it*

KEY POINTS

- *Particle-fluid interaction above the collector of catching type precipitation gauges are studied*
- *An extensive wind tunnel experimental campaign was performed*
- *Characterization of the aerodynamic response is visualised by means of PIV measurements*
- *A dedicated setup was realised to release drops and detect their deviation close to the collector*

1 INTRODUCTION

In windy conditions the bluff body aerodynamics of catching type precipitation gauges, characterized by updraft, acceleration and development of turbulent fluctuations above the gauge collector, induces deviations in the trajectories of the approaching hydrometeors. Therefore, in general, a certain amount of undercatch is to be expected in precipitation measurements obtained from catching-type gauges.

Wind tunnel testing of the aerodynamics of precipitation gauges and windshields has been a suitable investigation tool in precipitation measurement studies since the early work of *Bastamoff & Witkiewitch* (1926), although *Jevons* (1861) already used a simple wind tunnel test using smoke trails from smouldering brown paper to support his explanation of the wind exposure problem. Most studies concentrated mainly on identifying optimal design solutions to minimise the airflow acceleration and updraft and therefore the impact of the gauge body on the surrounding wind field. For example, *Sanuki et al.* (1952) tested two types of wind shields for rain gauges (conical and hollow ring-shaped designs) both in a water tank and in the wind tunnel. The flow around the funnel and wind shield was visualized by means of short, black and white wool strings tied to the main positions of the model. Further, air speed measurement was done at a position of 0.5 diameters above the funnel mouth. The flow patterns were photographed by means of aluminium powder spread over the water surface of the tank, or wool strings tied to the model in the wind tunnel. Only the airflow features were observed and visualized in these experiments, even if minimum generation of eddies at all parts of the flow was sought in the assessment of windshield design. *Warnik* (1953) visualized the airflow pattern above the gauge collector in wind tunnel tests by using titanium dioxide vapour as a tracer, introduced into the moist air passing through the tunnel to produce a dense white smoke. *Robinson & Rodda* (1969) examined four types of rain gauges in a wind tunnel using tuft indicators and smoke trajectories. The aerodynamics of two gauges with cylindrical shapes, one drop counter gauge characterized by bluff shape and a gauge with champagne glass shape, were studied. The authors concluded that the two gauges with cylindrical shapes appeared to produce the least satisfactory patterns of airflow, while the more complex shapes of the drop counter gauge and the champagne glass shape caused less distortion of the wind field.

Further to the characterization of the airflow field around the gauges some authors tried to capture the trajectories of water drops in a wind tunnel with the aim to measure their deformation close to the gauge and to estimate the wind induced undercatch. *Warnik* (1953) used real and sawdust snow injected into the tunnel to test the collection performance of both shielded and unshielded precipitation gauges. Photographs taken against a grid work background were used to measure the drift angle and velocity of undisturbed particles in the absence of the gauge so as to infer the theoretically true catch of an imaginary horizontal area equal to the area of the gauge orifice. *Green & Helliwell* (1972), visualized in the wind tunnel trajectories of drops of diameter 1.2, 2.2 and 3.5 mm, for wind speed between 1 and 10 ms^{-1}. The drop diameter was estimated using three control procedures in stagnant air, therefore the wind effect on the detachment of drops from the generating apparatus was not taken into account. The experimental measurements were conducted only on a gauge model with cylindrical shape, and drop trajectories were recorded with low details.

In the present work Wind Tunnel (WT) tests were performed in order to characterize the aerodynamic response of various gauge geometries and to detect the induced deviation of water drops trajectories. The measured flow velocity field and deviation of the drop trajectories were correlated by means of Particle Image Velocimetry (PIV) and optical techniques.

2 METHODOLOGY

Tests were conducted in the high speed and low turbulence section of the WT facility available at the Politecnico di Milano (GVPM). Three gauges with cylindrical, chimney and inverted conical shape were studied. PIV measurements were performed in the absence of drops in the flow in order to avoid any interference with the drop injecting instrumentation. The test chamber of the GVPM wind tunnel was uniformly filled with Castor oil smoke which was adopted as a passive tracer. A laser emitter was mounted to the ceiling of the test camber in order to illuminate a vertical section in the 2-D (x,z) plane, the surrounding environment was kept in the dark and the surface of the gauges was painted in black in order to avoid the reflection of light. A video camera was fixed in the tunnel on a rigid pole with its central axis normal to the stream-wise direction and centred on the middle of the lateral surface of the gauge collector. Wind speeds of 5 and 10 ms^{-1} were set. The effect of the different gauge geometries on the deviation of the approaching hydrometeors was investigated by realizing a dedicated setup able to generate and release water droplets in the incoming airflow and to precisely measure their trajectories when approaching the gauge collector. The wind tunnel was equipped with a hydraulic system to generate droplets, a high-speed camera and a high-power lamp to shot and illuminate droplets along their trajectories. To visualize the drop trajectories, the high-speed camera was placed in front of the gauge with its central axis normal to the stream-wise direction. The camera lens and the distance from the gauge collector were optimised so as to increase the resolution of the captured drop images without affecting the airflow field near the target. The plane of focus was set as the vertical plane passing through the central along-wind section of the gauge collector and the recording speed of the camera was set to 1000 fps, with an image resolution of 1600x900 pixels, the dimension of the image was 40 x 20 cm with a pixel size of 0.2370 mm. In each frame, the observed drop appears in a fixed position which evolves in the next frame. The video acquisitions were post-processed and from the time interval between two subsequent images and the conversion rate from pixels to millimeter the drop velocity in the 2-D shooting plane was derived. Additional details about the experimental setup and the images processing are reported in the work of *Cauteruccio et al.* (2020).

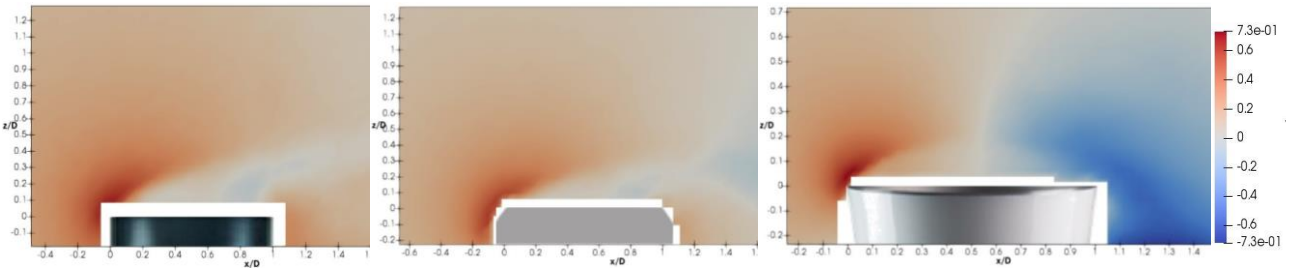

Figure 1. PIV fields of the normalized vertical velocity component in the central (y/D=0) stream-wise section, for chimney, cylindrical and inverted conical gauges at a wind speed of 10 ms^{-1}.

3 RESULTS

The PIV derived airflow velocity maps of the normalized vertical velocity component for the three investigated geometries are shown in Figure 1. Consistently with the work of *Cauteruccio et al.* (2019), for the inverted-conical gauge in uniform free-stream conditions, the updraft in the upwind part of the collector and the downdraft in the downwind part (Figure 1, panel 3) are comparable in magnitude. For the other cylindrical and chimney shaped geometries (Figure 1, panel 2 and 1 respectively) the region above the collector is almost totally affected by updraft components, although the cylindrical gauge shows lower updraft values than the other two geometries. Figure 2 reports the normalized positions of the maximum velocity values derived from PIV measurements for a wind speed of 5 ms^{-1} and reveals that these positions are higher and more dispersed for the chimney shaped gauge, while they are lower and more bounded for the

inverted conical shape. The behaviour of the cylindrical gauge is intermediate. Moreover, it was observed that the normalized magnitude of flow velocity is higher for the gauge with inverted conical shape and lower for the other two geometries. The comparison between measurements obtained at 5 and 10 ms^{-1} for the chimney-shaped gauge revealed that the maximum velocity patterns are not scalable both in terms of normalized velocity magnitude and positions.

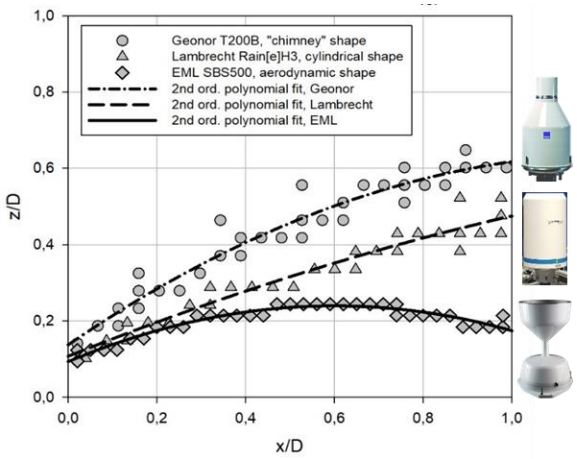

Figure 2. Normalized positions of the maximum velocity values obtained by means of PIV measurements for the wind speed of 5 ms^{-1}, for the chimney (circles), cylindrical (triangles) and inverted conical (diamonds) shapes, in the central (y/D =0) stream-wise section. The upwind edge of the collector is in (0,0).

Gauge shape and diameter D [m]	ID	Wind [ms^{-1}]	x/D	z/D
Cylindrical, D=0.160	L31	12.10	-1.3806	-0.26418
Chimney, D=0.160	G11	11.40	-1.31926	-0.29778
Inverted conical, D=0.252	S83	11.16	-0.79748	-0.27044

Table 1. Starting position, wind speed and identification codes for the three analysed drop trajectories and the associated gauge geometry.

Three observed drops trajectories, which in undisturbed conditions should hit the downwind part of the gauge collector but are deviated by the aerodynamic response of each geometry investigated, are shown and compared in Figure 3, panels a, b and c. Furthermore, the disturbed trajectories are commented in relation with the PIV velocity field just described above. Each observed drop trajectory was elaborated by linearly interpolating the positions associated with the undisturbed part of the trajectory, while the disturbed one was fitted with a third order polynomial. The threshold between the undisturbed and disturbed part of the trajectories was obtained by adopting a trial and error procedure with the objective to ensure the continuity of the slope curves (z/x, Figure 3, panel d) obtained as the first derivative of the fitted trajectories. The compared drop trajectories were chosen by minimizing the relative differences between the respective starting positions and the free-stream airflow velocity. These information are listed in Table 1. The parameters of the best-fit curves, which describe the trajectories of the droplets, and the associated correlation factors (R^2) are listed in Table 2. The collectors of the cylindrical and chimney shaped gauges have the same dimensions, while the collector of the inverted conical shape gauge is larger. The injection system was maintained at a fixed distance from the center of the gauge collector, therefore the droplets were released closer to the gauge for the inverted conical shape than for the other two gauges.

In Figure 3, panel (c) the trajectory of a drop travelling above the inverted conical gauge is depicted. The effect of the comparability between the airflow updraft and downdraft for the gauge with inverted conical shape, discussed above, can be observed here by noting that the deviation of the drop trajectory is almost totally bounded within the region delimited by the projection of the collector edges (x/D = ± 0.5, Figure 3, panel d, light grey line). In panels (a) and (b) the observed trajectories of drops which travel above the collector of the chimney-shaped and cylindrical gauges are depicted while their slopes are shown in panel (d) in black and dark grey lines. When approaching the gauge collector drops deviate from the undisturbed trajectory (dashed lines) and their slope decreases. In both cases, the drops fall outside instead of inside of the collector, therefore highlighting the very nature of the wind-induced undercatch affecting precipitation measurements.

Consistently with the PIV velocity field, the slope of the trajectory in the downwind part of the collector, for the cylindrical gauge increases faster than for the chimney shaped gauge. Moreover, the wind speed for the trajectory that travels above the collector of the chimney shaped gauge (U_{ref} = 11.4 ms^{-1}) is lower than for the trajectory captured above the cylindrical gauge (U_{ref} = 12.1 ms^{-1}). These results confirm that the aerodynamic response of the chimney shaped gauge is the most impactful on the collection performance of the gauge.

ID	m	Q	R2	a	b	C	D	R2
L31	0.1411	-0.0711	0.997	0.0293	0.0223	0.1133	-0.0921	0.9981
G11	0.1733	-0.0681	0.9985	0.0263	0.0138	0.1301	-0.0995	0.9998
S83	0.1991	-0.111	0.9965	0.0504	0.0100	0.1495	-0.1329	0.9999

Table 2. Parameters of the linear regression (m and q) for the undisturbed trajectories and of the third order polynomial for the disturbed ones (a, b, c and d), with the associated correlation factor.

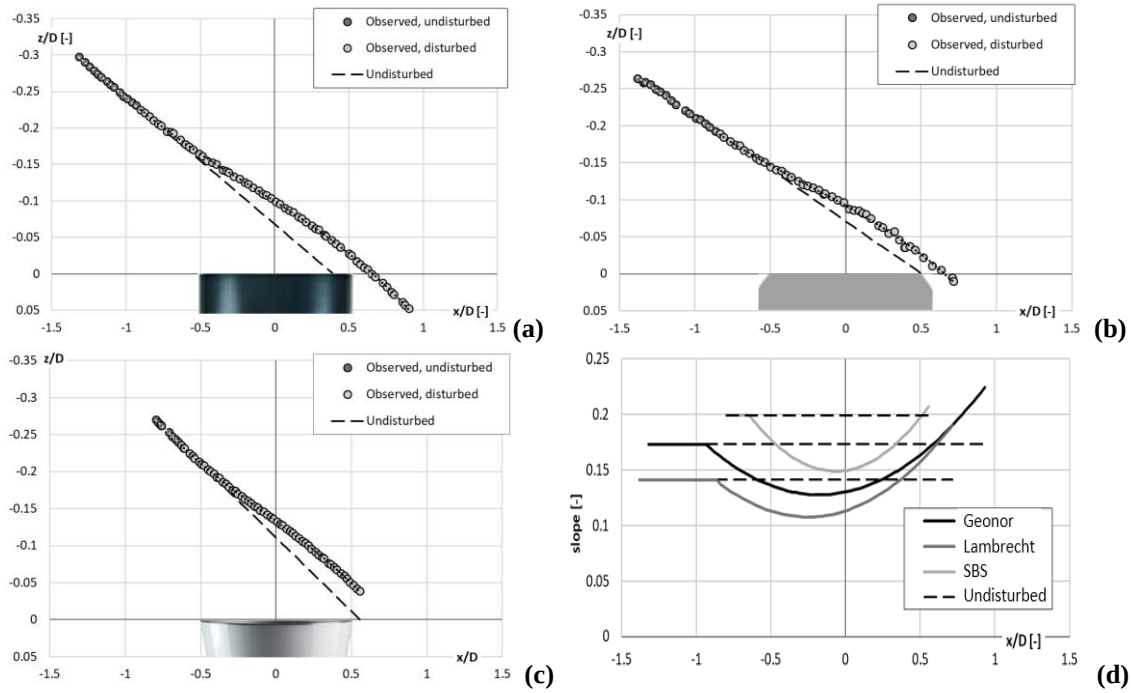

Figure 3. Observed (circles) and undisturbed trajectories (dashed line) of drops traveling above the collector of the gauges with chimney, cylindrical and inverted conical shape (panels a, b and c) and comparison between their slope curves (panel d).

Acknowledgements

This work was developed in the framework of the Italian national project PRIN20154WX5NA "Reconciling precipitation with runoff: the role of understated measurement biases in the modelling of hydrological processes".

REFERENCES

Bastamoff, S.L. & Witkiewitch, W.J. Les spectres aerodynamiques des pluviometres. Bull. Geophysique de L'Institut des Recherches Geophyssiqes, 1926, n.10, Moscow.

Cauteruccio A., Colli, M., Freda, A., Stagnaro, M. & Lanza, L.G. The role of the free-stream turbulence in attenuating the wind updraft above the collector of precipitation gauges. J. Atmos. Oceanic Technol., 2019, (in press).

Cauteruccio, A., Stagnaro, M., Brambilla, E., Lanza, L.G. & Rocchi, D. Wind tunnel validation of a particle tracking model to assess the wind-induced undercatch of rainfall gauges. XXXVII Convegno Nazionale di Idraulica e Costruzioni Idrauliche, Reggio Calabria, Italy, 2020.

Green, M.J. & Helliwell, P. R. The effect of wind on the rainfall catch. Distribution of precipitation in mountainous areas. World Meteorological Organization, 1972, Rep. 326, Vol. 2, 27–46.

Jevons, W.S.: On the deficiency of rain in an elevated rain-gauge, as caused by wind. The London, Edinburgh, and Dublin Philosophical Magazine and Journal of Science, 1861, 21(4), 421–433.

Robinson, A.C. & Rodda, J.C. Rain wind and aerodynamic characteristics of rain-gauges. Meteorol. Mag., 1969, 98, 113-120.

Sanuki, M., Tsuda, N. & Kimura, S. Water tank and wind tunnel tests on rain gauge wind shield. Pap. Met. Geophys., Tokyo, 1952, 3, p.54.

Warnik, C.C. Experiments with windshields for precipitation gages. Trans. American Geophysical Union, 1953, 34(3), 379 – 388.